

APPLICATION OF A STEADY-STATE THREE-PHASE SIMULATOR TO INTERPRET FLOW EXPERIMENTS

G.A. Virnovsky, J. Mykkeltveit, and J.E. Nordtvedt

RF-Rogaland Research, Stavanger, Norway

Abstract

In this paper, we describe a simplified 1D three-phase simulator assuming steady-state flow conditions and its implementation to special core analysis.

The steady-state simulator accounts for viscous, gravitational and capillary forces and is more accurate than a multipurpose black oil simulator. At the same time it is much simpler and works significantly faster. In combination with a parameter estimation subroutine; it provides a powerful and flexible tool for both planning and interpretation of multiphase flow experiments performed under steady-state conditions. It makes it possible to interpret measurements with full account for capillary forces and also to incorporate various types of input information.

The developed software is used to determine three-phase relative permeabilities from simulated steady-state experiments with account for capillary effects. The estimates are compared with the true functions, and with the relative permeabilities determined by Darcy's law.

Introduction

Three-phase flow is often encountered in natural reservoirs containing oil, water and gas, and also in underground aquifers polluted with industrial wastes. A study of three-phase flow properties is therefore necessary to enhance oil recovery, e.g., by reinjection of the produced gas which becomes more and more popular in the North Sea, and also to solve the problems of remediation of ground water. In this concern special core analysis in three-phase flow gradually attracts more attention.

The steady-state technique is one of conventional methods applied in special core analysis to determine relative permeabilities. Since the classical paper [10] it was recognised that capillary forces significantly affect laboratory experiments though neglected in a standard interpretation procedure. In order to avoid inaccuracies resulting from capillary effects neglect generally two options exist: either to avoid them by using sufficiently high total rates (which is not always possible, e.g., in the case of chalk, where the fragile material may crack if a high flow rate is utilised), or to introduce the corrections taking into consideration capillary pressure.

An analytical approach to correct the steady-state measurements of relative permeabilities taking into account capillary forces has been reported in [11], [12]. A more general approach based on history matching of measured data with the simulated [4] facilitates determination of relative permeabilities from both equilibrium and transient flooding experiments also taking fully into account capillary pressure. In this work, we develop and implement a specialised steady-state three-phase simulator. The simulator is tailor-made for simulation of the steady-state condition, and is considerably faster than multi-purpose black-oil simulators. Through

solution of the inverse problem associated with steady-state data and the mathematical model of the experiment, we demonstrate that three-phase relative permeabilities can be determined utilising this simulator. The simulator also provide for an effective mean for planning of three-phase steady-state flooding experiments.

Formulation of the model

The three-phase steady state model was formulated as an extension of a similar two-phase one described in Refs. [2] and [14].

The system of equations describing three-phase flow under the assumptions that compressibility and solubility of phases is neglected, consists of a conservation law and the Darcy's law for each of the phases, two capillary pressure relationships, and a trivial relationship for the saturations:

$$\begin{aligned} \phi \frac{\partial S_i}{\partial t} + \frac{\partial u_i}{\partial x} &= 0, \quad i = 1, 2, 3 \\ u_i &= -\kappa(x) \frac{f_i(S_1, S_3)}{\mu_i} \left(\frac{\partial p_i}{\partial x} - \rho_i g_x \right), \\ p_2 - p_1 &= \pi_{21}(S_1), \quad p_3 - p_2 = \pi_{32}(S_3), \\ \sum_{i=1}^3 S_i &= 1. \end{aligned} \quad (1)$$

We assume for convenience that the phases are numbered with respect to wettability, so that index 1 corresponds to the most wetting phase (e.g., water), index 3 corresponds to the most non-wetting phase (gas), while index 2 is left for the intermediate wetting phase (oil).

Note that in the above formulation the capillary pressures are assumed to be functions of only one argument (saturation). This type of representation of three-phase capillary pressures is often used, see [1], and is implemented in some commercial simulators (e.g., *ECLIPSE*). Also, some experimental findings indicate such a relationship[9].

The phase pressures may be eliminated from Eq. (1) in a standard way giving a closed system of two equations for two unknown saturations.

$$\begin{aligned} \phi \frac{\partial S_1}{\partial t} + U \frac{\partial F_1}{\partial x} &= -\frac{\partial}{\partial x} \kappa \left[\frac{\lambda_1}{\lambda_r} (\lambda_2 + \lambda_3) \frac{\partial \pi_{21}}{\partial x} + \frac{\lambda_1}{\lambda_r} \lambda_3 \frac{\partial \pi_{32}}{\partial x} \right], \\ \phi \frac{\partial S_3}{\partial t} + U \frac{\partial F_3}{\partial x} &= \frac{\partial}{\partial x} \kappa \left[\frac{\lambda_3}{\lambda_r} \lambda_1 \frac{\partial \pi_{21}}{\partial x} + \frac{\lambda_3}{\lambda_r} (\lambda_1 + \lambda_2) \frac{\partial \pi_{32}}{\partial x} \right]. \end{aligned} \quad (2)$$

$$\begin{aligned} \frac{\partial U}{\partial X} &= 0, \quad U = \sum_{i=1}^3 u_i, \\ F_i &= \frac{\lambda_i}{\sum_{j=1}^3 \lambda_j} \left(1 + \frac{\kappa}{U} g_x \sum_{j \neq i}^3 \lambda_j \Delta \rho_{ij} \right), \quad \Delta \rho_{ij} = \rho_i - \rho_j, \quad \lambda_i = f_i / \mu_i, \quad i = 1, 2 \end{aligned} \quad (3)$$

Matrix form of the equations reads

$$\phi \frac{\partial \mathbf{S}}{\partial t} + U \frac{\partial \mathbf{F}}{\partial x} = \frac{\partial}{\partial x} (\kappa A \frac{\partial \mathbf{S}}{\partial x}), \quad (4)$$

where

$$\mathbf{S} = \begin{pmatrix} S_1 \\ S_3 \end{pmatrix}, \quad \mathbf{F} = \begin{pmatrix} F_1 \\ F_3 \end{pmatrix}, \quad A = \begin{pmatrix} -\frac{\lambda_1}{\lambda_t} (\lambda_2 + \lambda_3) \frac{d\pi_{21}}{dS_1} & -\frac{\lambda_1}{\lambda_t} \lambda_3 \frac{d\pi_{32}}{dS_3} \\ \frac{\lambda_3}{\lambda_t} \lambda_1 \frac{d\pi_{21}}{dS_1} & \frac{\lambda_3}{\lambda_t} (\lambda_1 + \lambda_2) \frac{d\pi_{32}}{dS_3} \end{pmatrix}. \quad (5)$$

A steady state three-phase flow can then be described by

$$U \frac{d\mathbf{F}}{dx} = \frac{d}{dx} (\kappa A \frac{d\mathbf{S}}{dx}). \quad (6)$$

By integration one obtains

$$U (\mathbf{F}(\mathbf{S}) - \mathbf{F}^0) = \kappa A(\mathbf{S}) \frac{d\mathbf{S}}{dx}, \quad (7)$$

$$\mathbf{F}^0 = \begin{bmatrix} F_1^0 \\ F_3^0 \end{bmatrix}, \quad F_i^0 = u_i / U.$$

Since

$$\det A = -\pi_1' \pi_3' \frac{\lambda_1 \lambda_2 \lambda_3}{\lambda_t}, \quad \pi_1' = \frac{d\pi_{21}}{dS_1}, \quad \pi_3' = \frac{d\pi_{32}}{dS_3}, \quad (8)$$

$\det A$ is never negative. It is zero on the boundaries of the triangle Δ_s defined by

$$\Delta_s = \{S_1, S_3 \mid S_1 \geq 0, S_3 \geq 0, S_1 + S_3 \leq 1\}, \quad (9)$$

where phase mobilities are zero. If the capillarity matrix A has a non-zero determinant an inverse matrix exists;

$$A^{-1} = \frac{1}{\det A} \begin{pmatrix} \frac{\lambda_2}{\lambda_t} (\lambda_1 + \lambda_2) \pi_3' & \frac{\lambda_1}{\lambda_t} \lambda_3 \pi_3' \\ -\frac{\lambda_3}{\lambda_t} \lambda_1 \pi_1' & -\frac{\lambda_1}{\lambda_t} (\lambda_2 + \lambda_3) \pi_1' \end{pmatrix}. \quad (10)$$

In case when the inverse matrix exists Eq. (7) may be rewritten as

$$\frac{d\mathbf{S}}{dx} = \frac{U}{\kappa} A^{-1} (\mathbf{F}(\mathbf{S}) - \mathbf{F}^0), \quad (11)$$

After substitution of Eq. (10) into Eq. (11) and some algebraic manipulations, one obtains the following (surprisingly simple) system of two ordinary differential equations describing steady state saturations distributions along the coordinate:

$$\begin{aligned} \frac{dS_1}{dx} &= -\frac{1}{\pi_1} \frac{U}{\kappa} \left[\frac{F_2^0}{\lambda_2} - \frac{F_1^0}{\lambda_1} + \frac{\kappa}{U} g_x \Delta\rho_{12} \right] \\ \frac{dS_3}{dx} &= \frac{1}{\pi_3} \frac{U}{\kappa} \left[\frac{F_2^0}{\lambda_2} - \frac{F_3^0}{\lambda_3} + \frac{\kappa}{U} g_x \Delta\rho_{32} \right] \end{aligned} \quad (12)$$

Simulation of steady-state floods

Saturation profiles are obtained by numerical solution of the system (12) with boundary conditions requiring continuity of the flowing phases at the outlet end. To solve the system a standard Runge-Kutta algorithm is applied. In addition, pressure profiles are calculated by numerical integration of the Darcy's law, Eq. (1).

The following numerical results are calculated for input data corresponding to chalk samples (see Table 1 and Figure 1).

Table 1: Rock and fluid data.

A [sq. cm]	10
L [cm]	10
k [md]	2
μ_1 [cP]	1
μ_2 [cP]	1.19
μ_3 [cP]	0.02

Three injection rates: 0.04, 0.4 and 4 cc/min were used. At each of the 3 total rates 15 fractional flows were specified at the injection end to evenly cover the whole admissible region, see Figure 2. Nevertheless the resulting average saturations in the core are not evenly distributed in the admissible saturation triangle Δ_s . The equilibrium average saturations strongly depend on the total injection rate, see Figure 3. At a low rate, 0.04 cc/min gas saturations for all cases are close to capillary equilibrium saturations, i.e., capillary pressure between gas and oil is close to zero. At higher rates only a few points corresponding to higher gas saturations appear in the saturation diagram, so that most of the saturation region Δ_s is not covered. This observation allows to conclude that three-phase steady-state experiments require careful planning in order to provide reliable data. Both total rate and fractional flows have to be selected taking into account capillary forces. This problem can be successfully solved in a very rapid manner by utilising the described above steady state numerical model.

Calculation of relative permeabilities by Darcy's law and by a parameter estimation technique

To determine relative permeability from the steady-state points, two approaches exists. One could neglect the capillary pressure, and estimate the relative permeabilities utilising Darcy's equation directly. The corresponding values of the saturation would then be found by material balance using separator readings or by integration of a measured saturation profile. This is the traditional approach utilised by several authors (see, e.g., [9]). Another approach is to utilise the three-phase steady-state simulator developed in the previous sections. However, the relative permeabilities can then not be determined directly, as the equation can not be inverted

explicitly for the relative permeability. Here we demonstrate how the relative permeabilities can be determined by solving the inverse problem associated with the steady-state simulator and the data.

We represent the relative permeability by a functional representation, and find the parameters so that the weighted sum of squared differences between measured and simulated data is minimised. To do so, we need a sufficiently flexible representation for the relative permeabilities. In the past, B-splines have successfully been utilised for estimating two-phase relative permeabilities. This type of representation has been shown effective for representing the true (although unknown) flow functions in the two-phase as well as three-phase cases (see, e.g., [8,5,13]). In the three-phase cases, however, the relative permeability will generally be a function of two saturation, that is, each function will represent a surface on a plot with two saturations. Bivariate tensor-product B-splines have successfully been utilised for representing such surfaces[3,6,7].

To determine the parameters in the tensor-product representation of the relative permeabilities, we solve the non-linear least-squares problem defined by

$$J(\bar{\beta}) = [\bar{y}^{cal}(\bar{\beta}) - \bar{y}^{obs}]^T W [\bar{y}^{cal}(\bar{\beta}) - \bar{y}^{obs}] \quad (13)$$

where $\bar{\beta}$ is the coefficients in the tensor-product B-spline expansion of the relative permeabilities and w is the weighting matrix. Eq. (13) is minimised subject to the linear inequality constraints

$$G\bar{\beta} \leq \bar{\beta}^c \quad (14)$$

G can be selected so that monotonic relative permeability functions results[7]. $\bar{y}^{cal}(\bar{\beta})$ and \bar{y}^{obs} are the data calculated by the simulator and the experimental data, respectively. The data utilised can be pressure drop, average saturation of two phases, and saturation profiles of two phases, or any combination thereof. The minimisation problem is solved using a trust-region based Levenberg-Marquardt algorithm. Note that both the relative permeability as well as capillary pressure functions may be estimated utilising this approach, as the steady-state equations upon which the simulator is based, depend on both relative permeability as well as capillary pressure. However in the numerical experiments which follows the capillary pressure functions are assumed to be known.

To demonstrate the feasibility of the approach, we present and discuss an example. From the experiments discussed in the previous sections, we generate 15 fractional flows for each rate, see Fig. 2. Assuming all other properties of the porous medium being known, we estimate the relative permeability of all three phases by utilising the above described approach. We also calculate the points corresponding to utilising Darcy's equation directly, neglecting the capillary pressure. The data are synthetic, i.e., are generated by the simulator. This is a very instructive way of testing a method, as the true functions will be known, and the error in the estimation can be evaluated directly. We utilise a quadratic tensor-product B-spline expansion with two knots in each direction for each of the three relative permeability functions, and calculate pressure drop and average saturations corresponding to the 15 fractional flows for each rate.

In our estimation procedure, we utilise the same partition for the relative permeabilities as we used in the generation of the data, that is, we are here not addressing the issue of bias errors (see discussion in [8]). With two knots in each direction and quadratic splines, a total of 25 parameters results for each surface. However, as some of these parameters only have support outside of the saturation region for which we have data (see Figure 3 and discussion in [7]), the

total number of parameters for all three functions is reduced to 27. These 27 parameters are estimated minimising Eq.(13) subjected to Eq.(14).

The results of the estimation is shown in Figures 4-6. Figures 7-9 show the true relative permeability surfaces. As we can see from the figures, the errors (for both water and gas) are quite low in the area for which we have data. For this particular case, the influence of the capillary pressure on the data may be low, as the pointwise calculation of relative permeabilities utilising Darcy's law do not differ significantly from our estimate. The absolute average deviation from the true value for the water, oil, and gas relative permeabilities in the points corresponding to the fractional flows utilised, is 0.01, 0.05, and 0.07, respectively for the Darcy points at total rate 0.4 cc/min. Except for gas relative permeability, the accuracy of the Darcy's interpretation increases as the total rate increases, the corresponding deviations are now 0.002, 0.003, and 0.07. Though the absolute error is not dramatically big in absolute value, the relative errors are; particularly the error in the relative permeability to gas. In this case the absolute error is close to the true value since the Darcy's interpretation gives strongly underestimated relative permeabilities values at low gas saturations where gas becomes the wetting phase. The reason for this is the high ratio of capillary/viscous forces for the gas phase due to low viscosity of gas. For the gas relative permeability, the results are improved by the parameter estimation technique.

Table 2: Gas relative permeability by parameter estimation at 4 cc/min.

Sw	Sg	Parameter estimation	TRUE	Darcy
0.01	0.17	1.68E-02	1.29E-01	1.02E-06
0.21	0.16	5.38E-03	6.77E-02	3.25E-07
0.30	0.16	2.95E-03	4.23E-02	2.58E-07
0.38	0.15	1.53E-03	2.22E-02	2.36E-07
0.59	0.16	3.86E-06	5.40E-05	3.05E-07
0.01	0.17	1.73E-02	1.30E-01	3.35E-03
0.24	0.16	4.54E-03	5.92E-02	9.57E-04
0.35	0.16	2.06E-03	2.88E-02	7.87E-04
0.58	0.34	1.26E-03	3.58E-04	3.25E-04
0.01	0.18	1.79E-02	1.32E-01	9.94E-03
0.30	0.17	3.26E-03	4.36E-02	2.46E-03
0.57	0.37	3.67E-03	8.05E-04	7.43E-04
0.01	0.18	1.88E-02	1.34E-01	2.93E-02
0.55	0.40	6.70E-03	1.88E-03	1.73E-03
0.32	0.48	5.06E-02	7.55E-02	6.55E-02

Much work remains with this method; we need to investigate how higher capillary pressures will influence the estimation, what impact experimental errors will have on the estimation, as well as demonstrate the methodology on real experimental data. Also, we will investigate inclusion of saturation profiles on the accuracy with which the functions may be estimated. A particular strength of this method is that all previously reported steady-state data may be reinterpreted with this method, as the only inputs are the fractional flows along with average saturation and pressure drops. Hence, we do not require all details connected with experimental set-up or the transient data.

Conclusion

A three-phase, 1-D steady state numerical model taking into account capillarity has been developed. Its usefulness to interpret steady-state core floods has been demonstrated by way of numerical experiments.

Acknowledgements

The work has been supported by the Norwegian Research Council through our Strategic Institute Program within Advancing System and Parameter Identifications.

Nomenclature

Λ	=	capillarity matrix
\mathbf{F}	=	fractional flow vector function
F^0	=	fractional flow, a constant vector defined in Eq. (7)
g	=	acceleration of gravity
k	=	relative permeability
p	=	pressure
S	=	saturation
t	=	time
u	=	individual phase velocity
U	=	total Darcy velocity
x	=	coordinate
Δ	=	increment
Δ_s	=	admissible saturation region defined in Eq. (9)
ϕ	=	porosity
κ	=	absolute permeability
λ	=	mobility
μ	=	viscosity
π	=	capillary pressure
ρ	=	density

References

- [1] Aziz, Kh., Settary, A.: *Petroleum reservoir simulation*. Applied science publishers, London. pp. 29-38.
- [2] Dale, M., Ekrann, S., Mykkeltveit, J., Virnovsky, G. "Effective relative permeabilities and capillary pressure for 1D heterogeneous media." Presented at the 4th European Conference on the Mathematics of Oil Recovery. Røros, Norway 1994.
- [3] Mejia, G.M., Watson, A.T., Nordtvedt, J.E.: "A Method for Simultaneous Estimation of Three-Phase Relative Permeability and Capillary Pressure Functions," *AIChE Journal*, in press.

- [4] Nordtvedt, J. E., Urkedal H., Watson, A.T., Ebeltoft, E., Kolltveit, K., Langaas, K., and Øxnevad, I.E.I.: "Estimation of Relative permeability and capillary pressure functions using transient and equilibrium data from steady-state experiments". Presented at the International Symp. of the SCA, Stavanger, Norway, Sept., 1994.
- [5] Nordtvedt, J.E., Mejia, G., Yang, P., Watson, A.T.: "Estimation of Capillary Pressure and Relative Permeability Functions From Centrifuge Experiments," *SPE Reservoir Engineering*, Vol. 8, No. 4, Nov. 1993, pp. 292-298.
- [6] Nordtvedt, J.E., Ebeltoft, E., Iversen, J.E., Sylte, A., Urkedal, H., Vatne, K.O., Watson, A.T.: "Determination of Three-Phase Relative Permeabilities From Flooding Experiments," paper SPE 36683, *proceedings of the 71th ATCE 96*, Denver, USA, October 6-9, 1996, to appear.
- [7] Nordtvedt, J.E., Langaas, K., Sylte, A., Urkedal, H., Watson, A.T.: "Estimation of Three-Phase Relative Permeability and Capillary Pressure Functions," *proceedings of the fifth European Conference on the Mathematics of Oil Recovery (ECMOR V)*, Leoben, Austria, September 3-6, 1996.
- [8] Kerig, D.P., Watson, A.T.: "A New Algorithm for Estimating Relative Permeabilities From Displacement Experiments," *SPE Reservoir Engineering*, Vol. 2, 1987, 103.
- [9] Oak, M.J.: "Three-Phase Relative Permeabilities of Water-Wet Berea," *proceedings of the SPE/DOE Symposium on Enhanced Oil Recovery*, Tulsa, USA, 1990.
- [10] Richardson, J.G., Kerver, J.A., Hafford, J.A., and Osoba, J.S.: "Laboratory Determination of Relative Permeability", *Trans. AIME*, 195 (1952) 187-196.
- [11] Virnovsky, G. A., Guo, Y., Skjæveland S.M.: "Relative permeabilities and capillary pressure concurrently determined from steady-state experiments." *Proc. of the 8-th European Symp. on IOR*, 15-17 May 1995, Vienna, Austria, 1, p.60-69.
- [12] Virnovsky G.A., Skjæveland S.M., Surdal J., Ingsoy P., SPE 30541. "Steady-state relative permeability measurements corrected for capillary effects" Presented at the SPE Annual Conference in Dallas, USA, 22-25 Oct. 1995.
- [13] Watson, A.T., Richmond, P.C., Kerig, P.D., Tao, T.M.: "A Regression-Based Method for Estimating Relative Permeabilities From Displacement Experiments," *SPE Reservoir Engineering*, Vol. 3, 1988, 953.
- [14] Yortsos Y.C., Chang J. "Capillary effects in steady-state flow in heterogeneous cores." *Transport in porous media* 5. p. 399-420, 1990

Figures

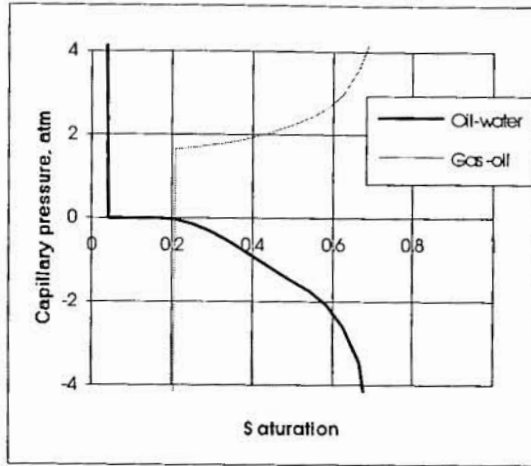


Figure 1: Oil-water and Gas-oil capillary pressure curves used in the simulations.

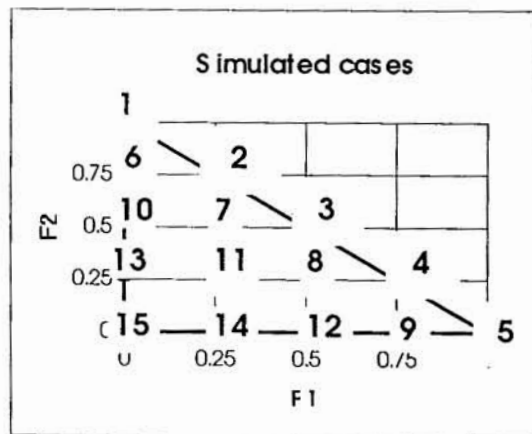


Figure 2: Case number and corresponding fractional flow at injection.

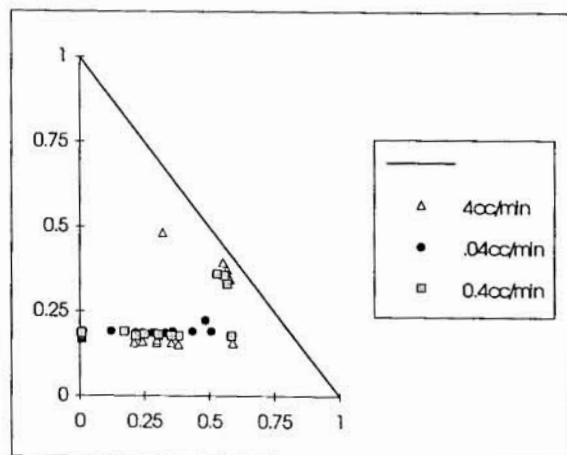


Figure 3: Average saturations in the core at different total rates.

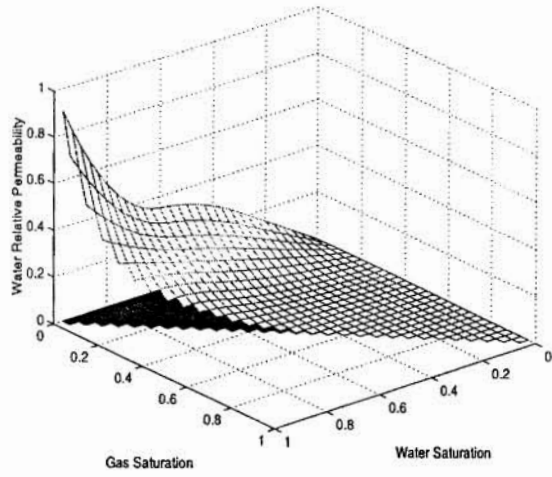


Figure 4: Estimated relative permeability to water.

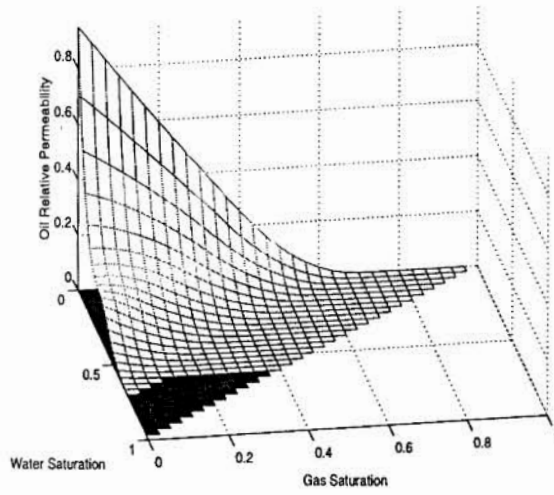


Figure 5: Estimated relative permeability to oil.

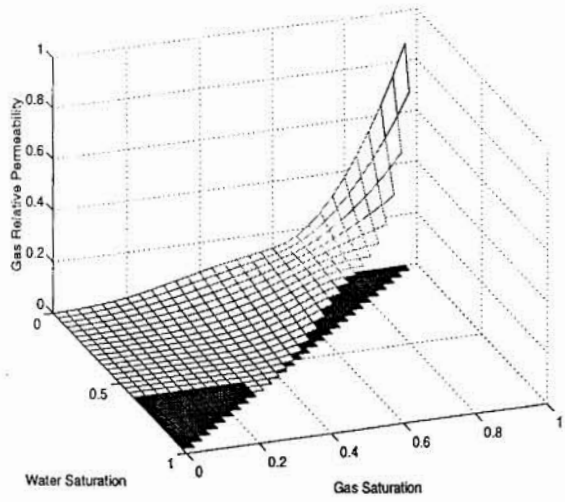


Figure 6: Estimated relative permeability to gas.

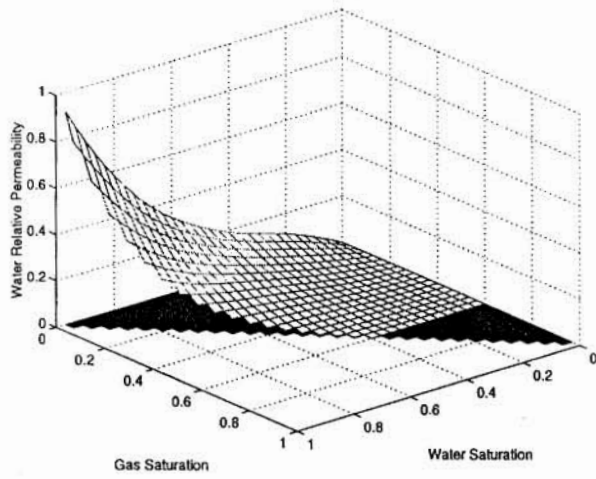


Figure 7: True relative permeability to water

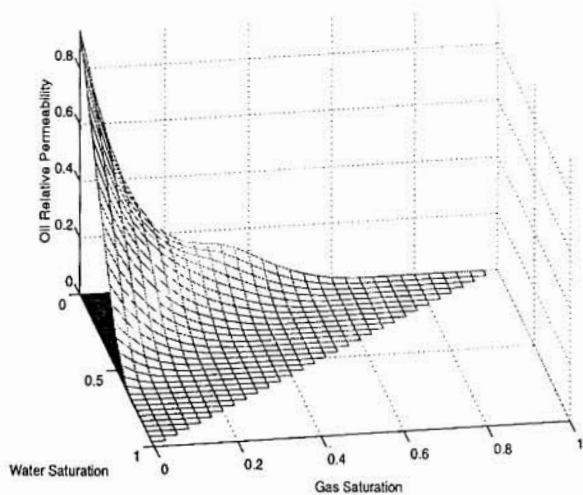


Figure 8: True relative permeability to oil.

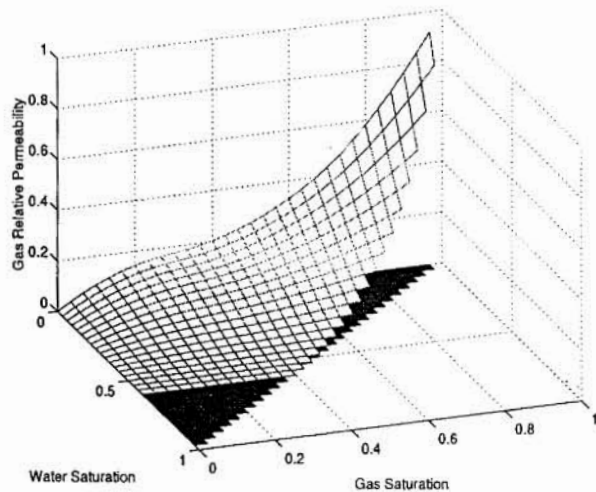


Figure 9: True relative permeability to gas.